Eighth Australasian Fluid Mechanics
Conference, University of Newcastle,
N.S.W., 28 November/2 December 1983.

APPLICATION OF THE DORODNITSYN BOUNDARY LAYER FORMULATION TO TURBULENT COMPRESSIBLE FLOW

R.W. FLEET AND C.A.J. FLETCHER

DEPARTMENT OF MECHANICAL ENGINEERING

UNIVERSITY OF SYDNEY, SYDNEY, N.S.W. 2006 AUSTRALIA

SUMMARY Dorodnitsyn spectral and Dorodnitsyn finite element boundary layer methods are compared with a representative finite difference package, STAN5, for two compressible turbulent aerofoil flows featuring severe adverse pressure gradients. The Dorodnitsyn methods are more accurate and the Dorodnitsyn finite element method is considerably more economical than STAN5.

1 INTRODUCTION

The Dorodnitsyn boundary layer formulation offers the following advantages:

(i) Solutions are obtained in (ζ, u) space rather than (x, y) space. This replaces an infinite domain in y by a finite domain in u (i.e. $o \leq u \leq 1$).

(ii) A uniform grid in the u - direction automatically follows downstream boundary layer growth.

(iii) A uniform grid in the u - direction gives high resolution, in physical space, close to the wall. This is particularly relevant for turbulent boundary layer flows.

(iv) The normal velocity, v, does not appear explicitly in the formulation, but can be recovered afterwards if required. Hence, only one equation is solved for two-dimensional flow.

(v) By treating a non-dimensional velocity gradient parameter as the dependent variable, the skin friction is computed very accurately.

The Dorodnitsyn boundary layer formulation is particularly effective in both a global (spectral) and a local (finite element) context for both laminar and turbulent incompressible flows (Fleet and Fletcher, 1982; Fletcher and Fleet, 1983a, 1983b).

For turbulent incompressible flow, comparisons with a typical finite difference package, STAN5 (Reynolds, 1976), indicate that the Dorodnitsyn spectral formulation (DOROD-SPEC) is very accurate and the Dorodnitsyn finite element formulation (DOROD-FEM) is very economical. Typically DOROD-FEM is ten times more economical than STAN5 while producing solutions of comparable accuracy (Fletcher and Fleet, 1983b).

Here we extend the basic Dorodnitsyn formulation to accommodate compressible flows by introducing a modified Stewartson transformation. The resulting Dorodnitsyn boundary layer method, in both the spectral and finite element forms, is then applied to two representative compressible turbulent (aerofoil) flows provided by Deiwert (1976) and Cook et al (1979). Both flows feature severe adverse pressure gradients.

The Dorodnitsyn spectral (DOROD-SPEC) and Dorodnitsyn finite element (DOROD-FEM) formulations are described in Section 2. In Section 3 results for skin friction and displacement thickness etc, obtained using DOROD-SPEC, DOROD-FEM and STAN5, are presented and compared for the two aerofoil flow cases.

2 DORODNITSYN FORMULATION

The Stewartson transformation is introduced to remove the explicit appearance of density in the compressible boundary layer equations. This is achieved by defining new independent variables

$$x_i = \int_o^{x_c} (P_e/P_\infty)(a_e/a_\infty)\,dx' \quad , \qquad (1)$$

$$y_i = (a_e/a_\infty) \int_o^{y_c} \rho/\rho_\infty \, dy' \quad ,$$

and dependent variables,

$$u_i = (a_\infty/a_e)u_c$$

$$\text{and } v_i = (P_\infty/P_e)(a_\infty/a_e)^2 u_c(\partial y_i/\partial x_c)y_c + (P_\infty/P_e)(a_\infty/a_e)(\rho/\rho_\infty)v_c \qquad (2)$$

where P, ρ and a are pressure, density and sound speed, respectively. Subscripts i and c refer to incompressible and compressible; subscripts ∞ and e refer to freestream conditions and the boundary layer edge. The current interest is in transonic flows, therefore the assumptions of adiabatic conditions and constant total enthalpy are made. The resulting (after the Stewartson transformation) "incompressible" equations are (dropping the subscript i),

$$\partial u/\partial x + \partial v/\partial y = 0 \qquad (3)$$

$$\text{and} \quad u\partial u/\partial x + v\partial u/\partial y = u_e \partial u_e/\partial x + (1/R_L)\partial\,[(1 + \nu_T/\nu)\partial u/\partial y]/\partial y \qquad (4)$$

where R_L $(= u_\infty L/\nu)$ is the Reynolds number.

In eq. (4) $\nu_T\, \partial u/\partial y$ is introduced to represent the Reynolds shear stress. In the outer boundary layer region a Clauser model is used to represent ν_T. In the inner region a mixing length formulation with van Driest damping is used by DOROD-FEM to represent ν_T. DOROD-SPEC (in the inner region) relates ν_T to the Dorodnitsyn variable, u', using the Spalding/Kleinstein model. Tests with DOROD-FEM (Fletcher and Fleet, 1983b) indicated that the two inner region models for ν_T give similar results.

The Dorodnitsyn formulation introduces the variables

$$\zeta = \int_o^x u_e(x')dx' \ , \quad \eta = R_L^{\frac{1}{2}} u_e y \ , \quad u' = u/u_e \qquad (5)$$

A generalised weight function, $f_k(u')$, is combined with eqs. (3) and (4) in the following way,

$$\int_o^1 \{f_k \times \text{eq.(3)} + df_k/du' \times \text{eq.(4)}\}\, du' = 0 \ . \qquad (6)$$

If $f_k(1) = 0$, eq. (6) can be manipulated to give

$$\frac{\partial}{\partial\zeta}\int_o^1 \theta^* u' f_k du' = (\dot{u}_e/u_e)\int_o^1 \theta^*(1-u'^2)(df_k/du')du' + \int_o^1 \partial\{(1+\nu_T/\nu)T\}/\partial u'(\partial f_k/du')du' \ , \qquad (7)$$

where $T = 1/\theta^* = \partial u'/\partial\eta$ and $\dot{u}_e \equiv du_e/d\zeta$. Equation (7) has the structure of an ordinary differential equation for $\theta^*(\zeta)$ if the nature of $\theta^*(u')$ is specified. Different choices for $T(u')$, $\theta^*(u')$ and $f_k(u')$ produce spectral (Section 2.1) and finite element (Section 2.2) formulations. From now on the superscript ' is dropped from u'.

2.1 Spectral Formulation

The spectral formulation is based on constructing special orthonormal functions, $g_k(u)$, and using them in place of f_k in eq. (7) and in the solution for θ^*,

$$\theta^* = [1/(1-u)]\left\{b_o + \sum_i b_i g_i(u)\right\} \ . \qquad (8)$$

The construction of $g_k(u)$ and the connection with the Dorodnitsyn functions, f_k, are described by Fletcher and Fleet (1983a).

Substitution of eq. (8) into eq. (7), and exploitation of the orthogonality condition produces the result

$$db_k/d\zeta = C_k - C_N(V_k/V_N) \ , \ k = 1, \ \ldots \ N-1 \qquad (9)$$

and $$V_N\, db_o/d\zeta = C_N, \qquad (10)$$

where $$C_k = (\dot{u}_e/u_e)\int_o^1 \theta^*(1-u^2)(dg_k/du)du - \left[(dg_k/du)/\theta^*\right]_{u=0} - \int_o^1 (d^2g_k/du^2)\qquad (1+\nu_T/\nu)T\ du \qquad (11)$$

and $$V_k = \int_o^1 g_k(u)\{u/(1-u)\}du \ . \qquad (12)$$

Equations (9) and (10) are explicit ordinary differential equations for the coefficients, b_o to b_{N-1} in eq. (8). For the results presented in Section 3, eqs. (9) and (10) have been integrated using the variable-order, variable-step Gear's method, with six unknown coefficients in eq. (8). The integrals in eqs. (11) and (12) have been evaluated using seven-point Gauss quadrature over the inner and outer regions (as defined for ν_T) of the boundary layer.

2.2 Finite Element Formulation

A modified Galerkin formulation (Fletcher, 1983a) is produced by introducing trial solutions,

$$\theta^* = \sum_j \{N_j(u)/(1-u)\}\theta_j(\zeta) \qquad (13)$$

$$(1+\nu_T/\nu)T = \sum_j \{(1-u)N_j(v)\}\ (1+\nu_T/\nu)_j \tau_j(\zeta) \qquad (14)$$

and setting $f_k = (1-u)N_k(u)$, $\qquad (15)$

where $N_j(u)$ are linear, one-dimensional shape functions. The form of eq. (14) exploits the economy inherent in the group representation (Fletcher, 1983b). Substitution into eq. (7) produces a system of ordinary differential equations,

$$\sum_j CC_{kj}\ d\theta_j/d\zeta = (\dot{u}_e/u_e)\ \sum_j EF_{kj}\theta_j + \sum_j AA_{kj}\tau_j \qquad (16)$$

$$k = 1, \ \ldots \ N \ .$$

The coefficients in eq. (16), like CC_{kj}, can be evaluated once and for all. The precise algebraic expressions are given by Fletcher and FLeet, 1983b. The system of equations, (16), is marched downstream using as non-iterative implicit algorithm that exploits the tridiagonal nature of eq. (16). For the results presented in Section 3 eleven equally-spaced points, spanning the boundary layer, have been used.

3. RESULTS AND DISCUSSION

Two test cases are considered. Firstly the transonic flow ($M_\infty = 0.7425$ and $R_L = 4 \times 10^6$) about an 18% circular arc aerofoil (Deiwert, 1976) is characterised by an adverse pressure gradient leading to separation close to the trailing edge. The second test case considers the transonic flow over an R.A.E. 2822 12.1% thick supercritical aerofoil ($M_\infty = 0.725$, $R_L = 6.5 \times 10^6$, $\alpha = 2.92°$). For this flow a severe local adverse pressure gradient occurs at about 65% chord associated with a shockwave (Cook et al, 1979).

TABLE 1 COMPARISON OF METHODS

CASE	METHOD	GRD. PTS. ACROSS B.L.	Δx/L	NO. OF STEPS, Δx/L
Adv. P.G. (Deiwert)	DOROD-FEM	11	0.001-0.009	612
	DOROD-SPEC	14	4(10-6)-0.084	568
	STAN5	37 - 45	0.001-0.033	682
SUPERCRITICAL (Cook et al)	DOROD-FEM	11	0.001-0.009	362
	DOROD-SPEC	14	8(10-6)-0.156	469
	STAN5	42 - 49	0.0004-0.055	533

The number of grid points across the boundary layer and the size and number of steps in the downstream direction for all three methods are shown in Table 1. For both DOROD-FEM and DOROD-SPEC the number of points across the boundary layer is about one quarter that required by STAN5 to obtain accurate solutions. This feature of Dorodnitsyn formulations, which contributes significantly to its economy, has been noted previously (Fletcher and Fleet, 1983b).

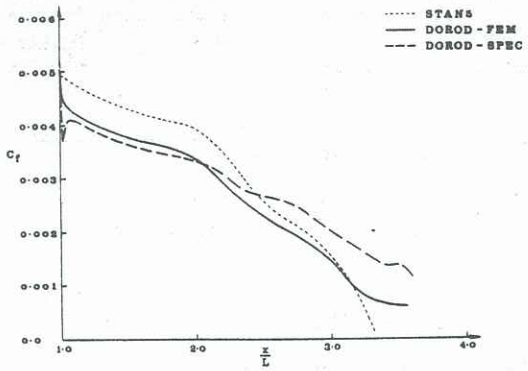

FIG. 1 Skin friction variation for adverse pressure gradient case.

3.1 Adverse Pressure Gradient Case

For this case, the local skin friction coefficient variation with downstream position is shown in Fig. 1. The DOROD-SPEC and DOROD-FEM results agree reasonably well with each other up to $x/L \approx 2.3$. Corresponding to the drop in the experimental pressure distribution for $x/L \gtrsim 2.3$, the results for these two methods diverge slightly with downstream position. For the DOROD-SPEC skin friction results, the 14 point distribution is in closer agreement with the DOROD-FEM results than the 10 point distribution (not shown). STAN5 overpredicts the DOROD-FEM results except for $x/L \geqslant 3.1$, where STAN5 is predicting an early separation.

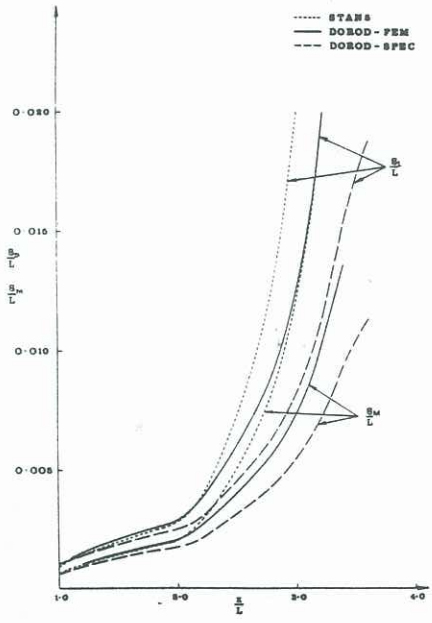

FIG. 2 Displacement and momentum thickness for adverse pressure gradient case.

The corresponding non-dimensional displacement and momentum thickness variations are shown in Figure 2. All three methods are in reasonable agreement up to $x/L \approx 2.1$ for both thicknesses. Beyond this position, STAN5 predicts a more rapid growth of both displacement and momentum thickness than as DOROD-FEM or DOROD-SPEC. Velocity profiles (not shown) are in close agreement for all three methods up to $x/L \approx 2.1$.

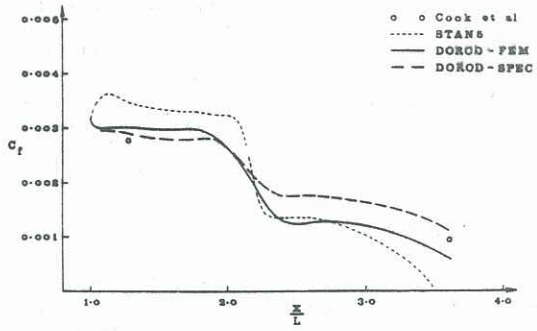

FIG. 3 Skin friction variation for the supercritical case.

3.2 Supercritical (Shockwave) Case

For this case skin friction values were deduced from the experimental velocity profiles by Cook et al (1979) and values upstream and downstream of the shock are shown in Fig. 3. Both DOROD-FEM and DOROD-SPEC give good agreement with the experimental friction results whereas STAN5 initially overpredicts the experimental skin friction and downstream of the shock underpredicts the skin friction. It is also clear that STAN5 is indicating a premature separation; this puts the behaviour of STAN5 for the adverse pressure gradient case (Diewert, 1976) in some doubt close to separation.

All three methods demonstrate the influence of the severe local adverse pressure gradient, due to the shockwave, on the skin friction distribution with STAN5 generally showing a steeper profile. The DOROD-SPEC results correspond to 14 grid points across the boundary layer in Table 1; solutions with 10 grid points across the boundary layer were less accurate but almost four times as economical.

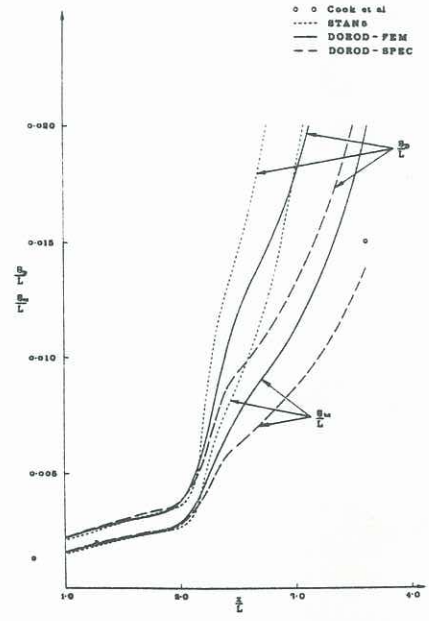

FIG. 4 Displacement and momentum thickness for supercritical case.

The corresponding non-dimensional displacement and momentum thickness variation with position is shown in Fig. 4. Experimental values for the momentum thickness (Cook et al, 1979) are indicated. It is clear from all the results that there is a rapid growth in both displacement and momentum thicknesses downstream of the shock. This rapid growth is predicted more closely by DOROD-SPEC and DOROD-FEM than by STAN5. However the implied rapid growth in boundary layer thickness weakens the assumption of a thin boundary layer implicit in the boundary layer equations. Velocity profiles (not shown) are in good agreement (between the different methods) up to $x/L \approx 2.0$.

4. CONCLUSION

The results for two test cases involving turbulent compressible boundary layers in adverse pressure gradients indicate that DOROD-SPEC and DOROD-FEM are more accurate than STAN5 particularly downstream of the shock-wave for flow over the supercritical aerofoil. As in the previous investigation of incompressible turbulent boundary layers (Fletcher and Fleet, 1983b) DOROD-FEM is significantly more economical than STAN5.

5. REFERENCES

COOK, P.H., McDONALD, M.A. and FIRMIN, M.C.P. (1979), Aerofoil RAE 2822 - Pressure Distributions, Boundary Layer and Wake Measurements, AGARD Adv. Rep. 138.

DEIWERT, G.S. (1976), Computation of Separated Transonic Turbulent Flows, AIAA J, 14, 735-740.

FLEET, R.W. and FLETCHER, C.A.J. (1982), A Comparison of the Finite Element and Spectral Methods for the Dorodnitsyn Boundary Layer Formulation, in Finite Element Methods in Engineering (ed. P.J. Hoadley and L.K. Stevens), Univ. of Melbourne Press, 59-63.

FLETCHER, C.A.J. (1983a), Computational Galerkin Methods, Springer-Verlag, New York.

FLETCHER, C.A.J. (1983b), The Group Finite Element Formulation, Comp. Meth. Appl. Mech. Eng., 37, 225-243.

FLETCHER, C.A.J. and R.W. FLEET (1983a), A Dorodnitsyn finite element formulation for laminar boundary layer flow, Int. J. Num. Meth. Fluids (to appear).

FLETCHER, C.A.J. and R.W. FLEET (1983b), A Dorodnitsyn Finite Element Formulation for Turbulent Boundary Layers, Computers and Fluids (to appear).

REYNOLDS, W.C. (1976), Computation of Turbulent Flows, Ann. Rev. Fluid Mechanics, 8, 183-208.